ISBN: 978-3-95450-202-8 doi:10.18429/JACoW-HB2018-WEA1WA02

APPROACHING THE HIGH-INTENSITY FRONTIER USING THE MULTI-TURN EXTRACTION AT THE CERN PROTON SYNCHROTRON

A. Huschauer, H. Bartosik, S. Cettour Cave, M. Coly, D. Cotte, H. Damerau, G. P. Di Giovanni, S. Gilardoni, M. Giovannozzi, V. Kain, E. Koukovini-Platia, B. Mikulec, G. Sterbini, F. Tecker, CERN, CH 1211 Geneva 23, Switzerland

Abstract

Complementary to the physics research at the LHC, several fixed target facilities receive beams from the LHC injector complex. To serve the fixed target physics program at the Super Proton Synchrotron, high-intensity proton beams from the Proton Synchrotron are extracted using the Multi-Turn Extraction technique based on trapping parts of the beam in stable resonance islands. Considering the number of protons requested by future experimental fixed target facilities, such as the Search for Hidden Particles experiment, the currently operationally delivered beam intensities are insufficient. Therefore, experimental studies have been conducted to optimize the Multi-Turn Extraction technique and to exploit the possible intensity reach. The results of these studies along with the operational performance of high-intensity beams during the 2017 run are presented in this paper. Furthermore, the impact of the hardware changes pursued in the framework of the LHC Injectors Upgrade project on the high-intensity beam properties is briefly mentioned.

INTRODUCTION

Since September 2015, the special beam extracted from the CERN Proton Synchrotron (PS) for the Super Proton Synchrotron (SPS) fixed-target physics programme has been generated using the so-called Multi-Turn Extraction (MTE) technique (see [1–4] for more detail). This peculiar extraction technique has superseded the Continuous Transfer (CT) process, proposed in 1973 [5], which occurs over five turns at 14 GeV/c to optimize the duty cycle by filling the SPS with only two subsequent extractions from the PS. The downside of the CT extraction is a significant amount of beam loss occurring at multiple locations around the ring [6], leading to high radiation dose to personnel during accelerator maintenance and repair, as well as to long cool down times.

MTE is a resonant extraction mechanism, which exploits advanced concepts of non-linear beam dynamics and is based on adiabatically crossing a stable fourth-order resonance to perform beam splitting in the horizontal phase space. The resulting beamlets - four islands and one core - are then extracted over five subsequent turns (see [7] for the detail of the implementation and [8] for the theoretical study on the trapping and splitting mechanisms).

The efficiency of the transverse splitting is defined as

$$\eta_{\mathrm{MTE}} = \frac{\langle I_{\mathrm{Island}} \rangle}{I_{\mathrm{Total}}}, \qquad (1)$$

where $\langle I_{\mathrm{Island}} \rangle$ and I_{Total} stand for the average intensity in each island and the total beam intensity, respectively. The nominal efficiency is 0.20, corresponding to an equal beam sharing between islands and core. This figure of merit is derived from the signal of the beam intensity measured in the transfer line joining the PS and the SPS.

An essential challenge encountered during the beam commissioning phase of this unique extraction technique had been the presence of significant fluctuations in η_{MTE}, caused by time-varying high-frequency ripples coming from power converters crucial for the operation of the PS [9].

To satisfy the requests of the SPS fixed-target experiments, the typical proton intensity per PS extraction has been in the range of $N_{\mathrm{p}} = 1.5 - 2 \times 10^{13}$ in the years 2015-17. Note that during the CERN Neutrinos to Gran Sasso [10] run, the typical proton intensity extracted from the PS was $N_{\mathrm{p}} \sim 2.6 \times 10^{13}$ with extraction losses at an average level of $\sim 7\%$ [6].

The summary of the overall MTE performance in terms of beam losses at the PS and SPS is shown in Fig. 1 where, for the sake of comparison, the typical CT performance is also reported. The overall reduction of losses along the accelerator complex over the years is clearly visible. Moreover, the main feature of MTE and the main reason for replacing CT is clearly visible, namely the drastic reduction of losses in the PS ring. In the transfer lines joining the two machines a mild improvement (over the years and with respect to CT) is also visible. The SPS performance is still slightly worse for MTE with respect to CT, although an improvement over the years is visible. Note that the main SPS performance limitation originates from the value of the delivered vertical emittance being at the limit of the machine acceptance, hence explaining the higher losses at injection.

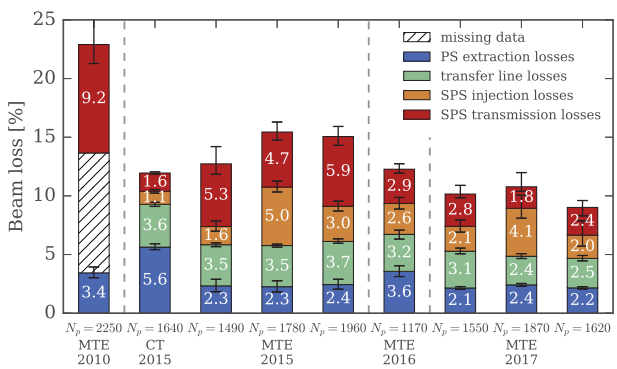

Figure 1: Summary of the beam losses for CT and MTE over the years. For each case the total beam losses are split into the various loss contributions occurring from the PS to the SPS.

ISBN: 978-3-95450-202-8 doi:10.18429/JACoW-HB2018-WEA1WA02

According to future proposals, like the Search for Hidden Particles (SHiP) experiment [11], much higher intensity, reaching up to $2.4 - 2.5 \times 10^{13}$ protons per PS extraction, might be required. In light of these potential needs, an intense experimental campaign has been carried out in 2017 to assess the actual MTE performance for these high-intensity beams. This has been considered an essential step in the formal process of declaring MTE a suitable and definite operational replacement of CT. Note that intensity-dependent effects had been observed with MTE already during its infancy [12] and the theoretical explanation, based on the analysis of indirect space charge effects, has been provided only recently [13].

This paper focuses on the results of the experimental campaign carried out during the whole 2017 PS and SPS proton run. A number of detailed parameter scans will be presented, which were crucial to start with a highly-optimised MTE beam of intermediate intensity. The discussion of the high-intensity tests follows later, including the various steps undertaken in the whole accelerator chain starting from the PS Booster (PSB) to the PS and the SPS.

PREPARATORY STUDIES

Overview of MTE

Figure 2 shows a sketch of the PS ring with the main non-linear magnets required for MTE, namely sextupoles and octupoles. While the sextupoles and the close-by octupoles are located in areas with maximum horizontal and minimum vertical β-functions to enhance their effect, the other distributed octupoles are located in areas with maximum vertical and minimum horizontal β-functions and are used to minimise the non-linear coupling between the two transverse planes [2–4].

The PS cycle for SPS fixed target beam production is shown in Fig. 3 (upper) together with the evolution of the strength of the non-linear magnets used to perform beam trapping and splitting (lower). It is worthwhile mentioning that a non-negligible boost to η_{MTE} is provided by the use of

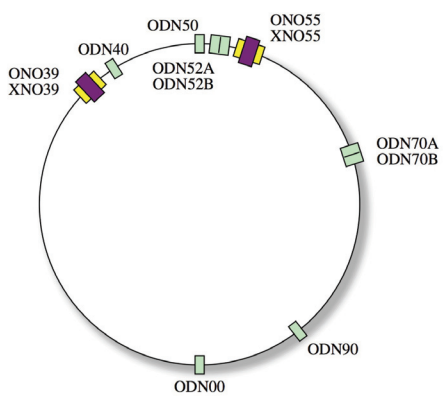

Figure 2: Sketch of the PS ring with the key elements of MTE, i.e. sextupole (called 'X') and octupole (called 'O') magnets.

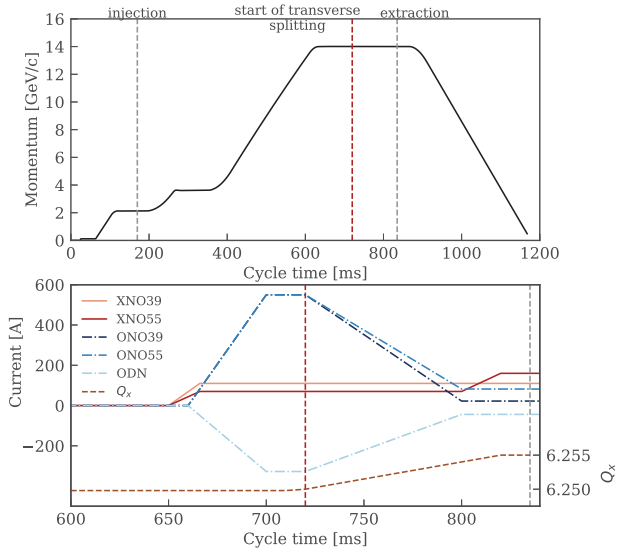

Figure 3: Upper: Sketch of the PS magnetic cycle with the main events. Lower: evolution of the strengths of the main MTE elements. The vertical dashed line indicates the moment of resonance crossing.

a horizontal dipolar excitation during the resonance-crossing process. Such an excitation is imparted by the transverse feedback (TFB) used in open loop and its impact has been analysed in detail in the past [4]. The important dependency of η_{MTE} on the excitation amplitude is shown in Fig. 4.

Transverse Excitation and Core Emittance

Extensive measurements of the transverse emittance of the beam injected in the SPS revealed a large emittance growth in the horizontal plane for the core. This observation triggered a number of investigations. In fact, the use of the transverse dipolar excitation is essential to achieve the nominal value of η_{MTE}. Nevertheless, the emittance growth could be a negative side effect of the excitation of core particles. This possibility has been verified by a detailed measurement campaign, where η_{MTE} and the horizontal emittance growth of the core have been measured as a function of the excitation frequency (see Fig. 5).

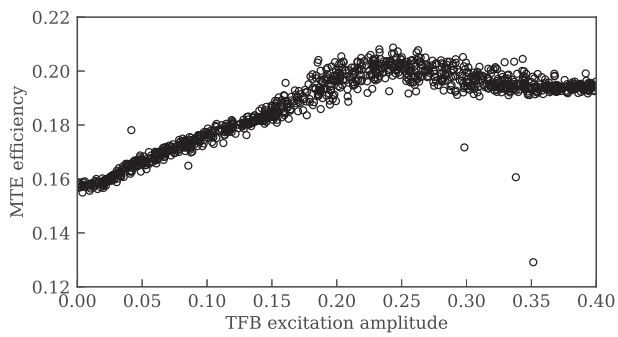

Figure 4: η_{MTE} as a function of the TFB excitation amplitude. Its beneficial impact on η_{MTE} is clearly visible together with a saturation effect.

ISBN: 978-3-95450-202-8 doi:10.18429/JACoW-HB2018-WEA1WA02

In the upper part, η_{MTE} shows a dip close to the resonant tune and then stabilises for higher values of the transverse feedback frequency. In the lower part, the emittance growth reveals a rather broad plateau where the emittance increase is smaller than 5%. The nice feature is that a relatively wide range of frequency values exists, for which η_{MTE} is large and constant, while the emittance growth is small. From an operational point of view this means that the transverse feedback can indeed be tuned to maximise its beneficial impact, while keeping the undesired impact on the core emittance under control. However, special care has to be taken when setting the parameters of the transverse feedback. Furthermore, the excitation frequency allows to optimize η_{MTE} to account for unavoidable drifts of the machine tune over time.

Optimisation of the Non-linear Magnets

The operational settings of the non-linear magnets shown in Fig. 3 (lower) have been defined to maximise η_{MTE} (by means of ONO39 and ONO55), to minimise the non-linear coupling between the two transverse planes (by means of the ODN family), and to reduce emittance dilution and extraction losses during the change of the islands' phase prior to extraction (by means of the XNO55 circuit) [4].

Nonetheless, some of the features of the time variation of the sextupoles and octupoles have been revised in view of the high-intensity tests. At first, the octupole circuits have been probed, in particular to assess whether their maximum strength or the slope from the maximum value at resonance crossing to the final one before extraction were optimal. The results of these scans in terms of distribution of measured η_{MTE} are shown in Fig. 6. A strong dependence on the value of the maximum strength is clearly observed, while a mild increase of the MTE efficiency is measured when the slope is reduced, i.e. the time variation and therefore the adiabaticity of the process is increased.

The impact of the maximum strength of the ODN magnets, which are meant to control the non-linear coupling between the two transverse planes has been probed too and the measurements show that η_{MTE} is essentially independent on the settings of the plateau of the current function of the ODN magnets.

As a final test, the strength of the sextupole XNO55 has been varied and its impact on the extraction losses measured by means of beam loss monitors (BLMs) and the results are reported in Fig. 7. The strength varied corresponds to the final stage of the resonance crossing process, i.e. when the islands are transported towards higher amplitude and their phase is changed in order to prepare for the extraction. This process had already been studied in detail during the first stages of the MTE commissioning and once more, careful setting of the sextupole XNO55 is shown to importantly impact the losses at extraction.

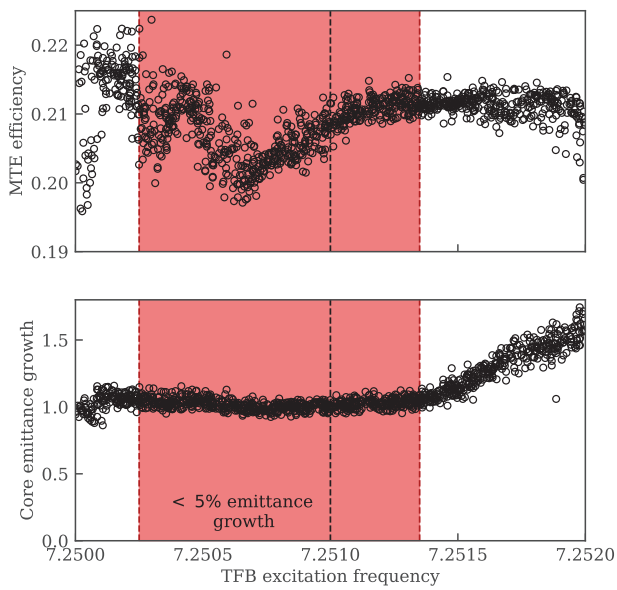

Figure 5: MTE efficiency (upper) and core emittance growth (lower) as a function of the excitation frequency of the TFB. The shaded area corresponds to an emittance growth of less than 5%. A tuning range compatible with high η_{MTE} and low core emittance growth is clearly visible.

HIGH-INTENSITY TESTS

General Considerations

The constraints on the transverse emittances for the MTE fixed target beams beam parameters are three-fold: firstly, the horizontal emittance received by the PS should be large to increase η_{MTE}; secondly, the vertical emittance should be as small as possible to overcome the acceptance issues in the SPS; thirdly, extraction losses at PSB should be kept low.

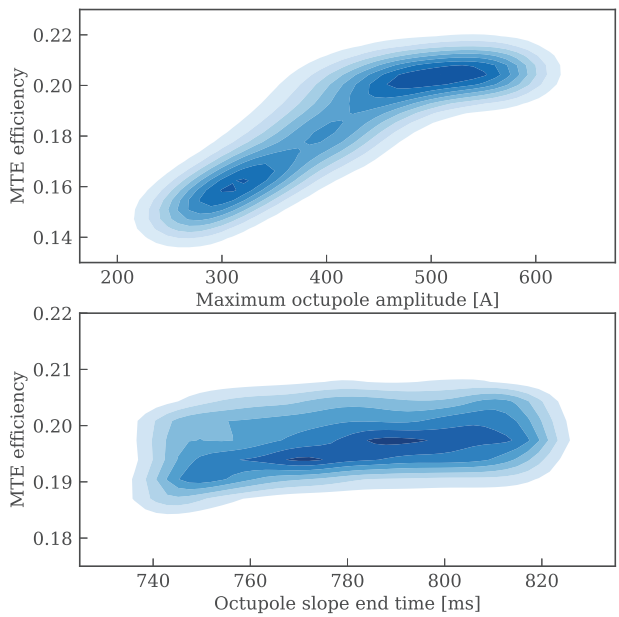

Figure 6: Distribution of efficiency as a function of the maximum strength of octupoles ONO39 and ONO55 (upper) and of their (lower). A strong dependence of η_{MTE} on the strength is visible, while the slope is affecting it only mildly.

ISBN: 978-3-95450-202-8 doi:10.18429/JACoW-HB2018-WEA1WA02

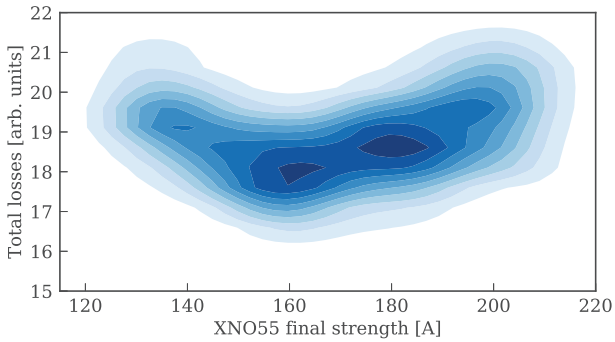

Figure 7: Distribution of extraction losses as a function of the final strength of the sextupole XNO55 during the separation of the islands and the rotation of their phase. A clear dependence is visible.

The high-intensity tests started with a careful preparation of the beam in the PSB. This machine is essential for defining the transverse emittances of the beam that will be transported through the chain to the SPS. Note that the horizontal emittance will be reduced by the splitting process at the PS, while the vertical one is essentially preserved due to the careful adjustment of the PS machine settings to linearly and non-linearly decouple the horizontal and vertical planes.

Satisfying simultaneously the emittance constraints has been a challenge for the PSB specialists, even more as high-intensity beams require to accumulate the injected beam from the Linac 2 over several PSB turns, which naturally increases the emittances. While this is certainly beneficial for the horizontal plane, it is a potential issue for the vertical one. In the end, however, this could be improved by optimizing the PSB working point at injection, which allowed to carry on with the optimization in the downstream accelerators.

PS Results

During the high-intensity tests, three main aspects have been scrutinised at the PS ring: firstly, the dependence of η_{MTE} on intensity; secondly the dependence of extraction losses on intensity; thirdly the beam behaviour in the longitudinal plane during the de-bunching applied after splitting and prior to beam extraction. The last point will not be dealt with in detail in this paper. It is only worth mentioning that no particular issue was observed and that the beam could be kept stable during the de-bunching even at high-intensity.

A comparison of the distribution of η_{MTE} for the operational beam in 2017 (typical intensity around $1.5-1.6\times10^{13}$ protons) and for that prepared for the high-intensity tests (typical intensity around 2.4×10^{13} proton) is shown in Fig. 8 (upper). The two distributions are very similar, featuring a rather similar median. The only difference is a larger tail skewed towards low values of η_{MTE} for the case of the high-intensity beam. This is not considered to be a fundamental issue as it could be fixed by working on the reproducibility of the intensity delivered by the Linac 2 and the PSB.

In fact, as it can be seen in Fig. 8 (lower), while η_{MTE} is practically constant for a wide range of beam intensities (essentially from the operational one and up to about 2.2×10^{13} protons), a small reduction is observed for the case of 2.4×10^{13} protons. Hence, a fluctuating beam intensity could explain the tail.

The second aspect considered during the tests has been the evolution of the beam losses at extraction, which is also a means to evaluate whether the transverse beam properties are changing with intensity. Figure 9 reports the losses at extraction as measured by fast BLMs, which are devices capable of providing the turn-by-turn losses with sub-turn sampling rate. Thus, they allow distinguishing between the losses for the islands (upper) and the core (lower).

The losses are shown as a function of intensity and are given for two key locations in the PS ring, namely the location of the so-called dummy septum [2–4] in straight section (SS) 15 and that of the magnetic extraction septum in SS16. It is worth mentioning that the lower losses for the core extraction are due to the faster rise time of the kickers, with respect to those used for the four islands. The important feature visible in the plots is that the increase of beam losses is to a large extent linear with intensity, thus indicating that no new phenomenon is appearing when intensity is increased.

SPS Results

The final step of the high-intensity studies has been the delivery of the optimised beam from the PS to the SPS. Due to a number of external constraints it has been decided to focus on the setting up of the first injection batch from the PS as a sort of proof of principle, leaving the complete setting up of both batches for later.

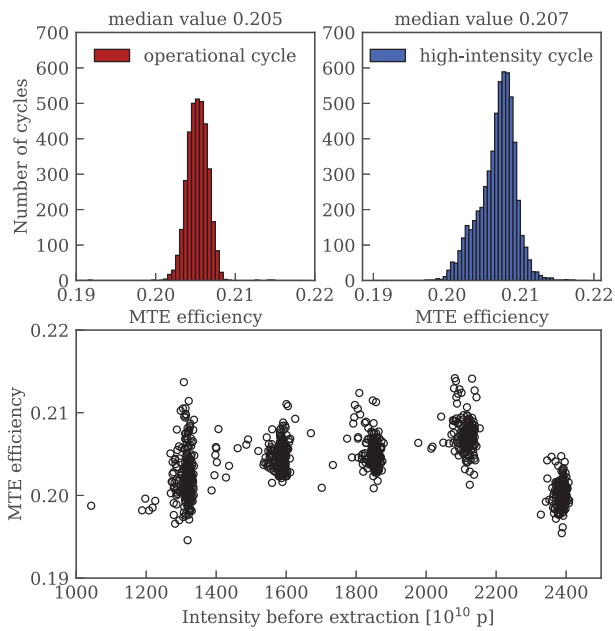

Figure 8: Upper: Distribution of MTE efficiency for the operational (left) and the high-intensity variant (right). The median of the distribution is essentially the same, while a low-efficiency tail is present for the high-intensity beam. Lower: MTE efficiency for various beam intensities.

ISBN: 978-3-95450-202-8 doi:10.18429/JACoW-HB2018-WEA1WA02

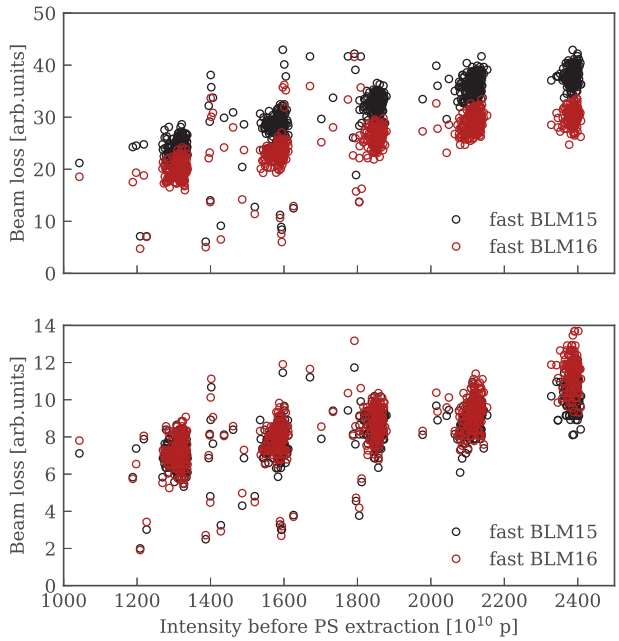

Figure 9: Measured extraction beam losses for the islands (upper) and core (lower) as a function of the total beam intensity. The losses are given in the extraction region, i.e. at the location of the dummy septum in SS15 and of the magnetic septum in SS16.

The main outcome of these tests is reported in Fig. 10 where the transmission through the various stages of the SPS cycle is shown. For the sake of precision, the performance of both injected batches from the PS is reported, but only the first one is meaningful in terms of possible performance-reach estimate. The transmission of the operational MTE beam is also reported for comparison. A reduction of transmission at injection is clearly visible for the high-intensity beam. This is mainly due to the increased value of the vertical emittance, which goes beyond the vertical SPS acceptance, and therefore dominates the performance at injection. In all further stages of the SPS cycle the high-intensity

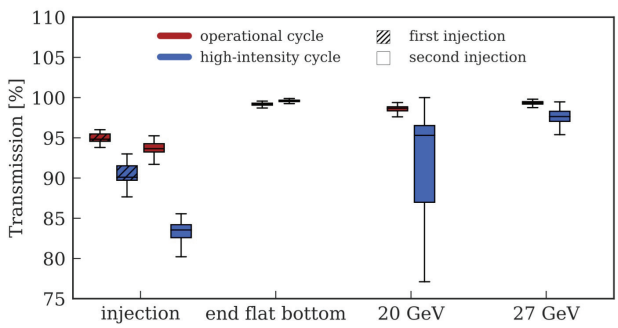

Figure 10: Beam transmission in the SPS between the various stages of its cycle. The data are split up for first and second injection into the SPS. It is worth stressing that a careful tuning could be performed only for the first PS injection.

beam performs similarly to the operational beam, at least the high-end part of the distribution of transmission values is comparable with that of the operational beam. It is worth mentioning that the transmission up to 20 GeV/c includes the start of acceleration as well as transition crossing, which requires careful adjustment of the machine parameters.

These results have been considered as a sign that the SPS can perform equally well with both beams (operational and high-intensity) as long as sufficient commissioning time is allocated and a smaller vertical beam emittance is provided by the PS. Reduced emittances will become available as the planned improvements of the LHC Injectors Upgrade (LIU) project at CERN [14] will be implemented during the Long Shutdown 2 (LS2) starting at the end of 2018.

CONCLUSIONS

MTE started operation in the second half of 2015, thus replacing the CT extraction mode. Since then, the MTE performance has been constantly improved, in particular in the SPS, hence approaching that of CT. It is worth stressing that the latter had gone through a series of optimisations and improvements based on decades of operational experience.

A high-intensity version of MTE has been produced in 2017 and tests were carried out in the PSB, the PS, and the SPS. At the PSB the main challenge has been the generation of the high-intensity beams with low extraction losses while fulfilling the constraints imposed on the transverse emittances by either the PS, i.e. a large horizontal emittance to optimise the MTE efficiency, or the SPS, i.e. a small vertical emittance to minimise the injection losses due to the vertical acceptance. This was successfully achieved, thus allowing to move to the downstream machines.

In the PS, the performance of high-intensity MTE beams is comparable with that of the operational beam. The SPS performance is dominated by the value of the vertical emittance delivered by the PS, where the emittance delivered by the PSB is preserved. The larger vertical emittance with respect to the nominal beam explains the larger losses observed. Considering this aspect, it is clear that the novel LIU beams will mitigate this limitation. All in all, in spite of the very limited set up time, no sign of hard obstacle to further improve the overall performance was found.

Based on the successful outcome of the tests carried out in 2017, it was formally decided to discontinue CT operation and to dismantle the corresponding hardware during LS2.

ACKNOWLEDGEMENTS

We would like to express our warm thanks to the operation crews of the PSB, the PS, and the SPS synchrotrons, who provided invaluable support during the experimental studies discussed in this paper.

REFERENCES

[1] R. Cappi and M. Giovannozzi, "Novel method for multiturn extraction: trapping charged particles in islands of phase space", *Phys. Rev. Lett.* vol. 88, p. 104801, 2002.

ISBN: 978-3-95450-202-8 doi:10.18429/JACoW-HB2018-WEA1WA02

[2] J. Borburgh , S. Damjanovic, S. Gilardoni, M. Giovannozzi, C. Hernalsteens, M. Hourican, A. Huschauer, K. Kahle, G. Le Godec, O. Michels, and G. Sterbini, "First implementation of transversely split proton beams in the CERN Proton Synchrotron for the fixed-target physics programme", *EPL*, vol. 113, p. 34001, 2016.

[3] S. Abernethy, A. Akroh, H. Bartosik, A. Blas, T. Bohl, S. Cettour-Cave, K. Cornelis, H. Damerau, S. Gilardoni, M. Giovannozzi, C. Hernalsteens, A. Huschauer, V. Kain, D. Manglunki, G. Métral, B. Mikulec, B. Salvant, J.-L. Sanchez Alvarez, R. Steerenberg, G. Sterbini, and Y. Wu, "Operational performance of the CERN injector complex with transversely split beams", *Phys. Rev. Accel. Beams*, vol. 20, p. 014001, 2017.

[4] A. Huschauer, A. Blas, J. Borburgh, S. Damjanovic, S. Gilardoni, M. Giovannozzi, M. Hourican, K. Kahle, G. Le Godec, O. Michels, G. Sterbini, and C. Hernalsteens, "Transverse beam splitting made operational: key features of the multi-turn extraction at the CERN Proton Synchrotron", *Phys. Rev. Accel. Beams*, vol. 20, p. 061001, 2017.

[5] C. Bovet, D. Fiander, L. Henny, A. Krusche, and G. Plass, "The fast shaving ejection for beam transfer from the CPS to the CERN 300 GeV machine", *IEEE Trans. Nucl. Sci.*, vol. 20, p. 438, 1973.

[6] J. Barranco García and S. Gilardoni, "Simulation and optimization of beam losses during continuous transfer extraction at the CERN Proton Synchrotron", *Phys. Rev. ST Accel. Beams*, vol. 14, p. 030101, 2011.

[7] M. J. Barnes, O. E. Berrig, A. Beuret, J. Borburgh, P. Bourquin, R. Brown, J.-P. Burnet, F. Caspers, J.-M. Cravero, T. Dobers, T. Fowler, S. Gilardoni, M. Giovannozzi (ed.), M. Hourican, W. Kalbreier, T. Kroyer, F. Di Maio, M. Martini, V. Mertens, E. Métral, K.-D. Metzmacher, C. Rossi, J.-P. Royer, L. Sermeus, R. Steerenberg, G. Villiger, T. Zickler, "The CERN PS multi-turn extraction based on beam splitting in stable islands of transverse phase space: Design Report", CERN-2006-011, 2006.

[8] A. Bazzani, C. Frye, M. Giovannozzi, and C. Hernalsteens, "Analysis of adiabatic trapping for quasi-integrable area-preserving maps", *Phys. Rev. E*, vol. 89, p. 042915, 2014.

[9] A. Huschauer, M. Giovannozzi, O. Michels, A. Nicoletti, G. Sterbini, "Analysis of performance fluctuations for the CERN Proton Synchrotron multi-turn extraction", *J. Phys.: Conf. Ser.*, vol. 874, p. 012072, 2017.

[10] K. Elsener, G. Acquistapace, J.-L. Baldy, A.E. Ball, P. Bonnal, M. Buhler-Broglin, F. Carminati, E. Cennini, A. Ereditato, V.P. Falaleev, P.E. Faugeras, A. Ferrari, G. Fortuna, L. Foà, R. Genand, A.L. Grant, L. Henny, A. Hilaire, K. Hübner, J. Inigo-Golfin, K.-H. Kissler, L.A. López-Hernandez, J.-M. Maugain, M. Mayoud, P. Migliozzi, D. Missiaen, V. Palladino, I.M. Papadopoulos, F. Pietropaolo, S. Péraire, S. Rangod, J.-P. Revol, J. Roche, P.R. Sala, C. Sanelli, G.R. Stevenson, B. Tomat, E. Tsesmelis, R. Valbuena, H.H. Vincke, E. Weisse, M. Wilhelmsson, "The CERN neutrino beam to Gran Sasso (NGS): conceptual technical design", CERN-98-02, INFN-AE-98-05, 1998.

[11] G. De Lellis, "Search for Hidden Particles (SHiP): A New Experiment Proposal", *Nucl. Part. Phys. Proceedings*, vol. 263-264, p. 71, 2015.

[12] S. Gilardoni, M. Giovannozzi, and C. Hernalsteens, "First observations of intensity-dependent effects for transversely split beams during multiturn extraction studies at the CERN Proton Synchrotron", *Phys. Rev. ST Accel. Beams*, vol. 16, p. 051001, 2013.

[13] S. Machida, C. Prior, S. Gilardoni, M. Giovannozzi, A. Huschauer, and S. Hirlander, "Numerical investigation of space charge effects on the positions of beamlets for transversely split beams", *Phys. Rev. Accel. Beams*, vol. 20, p. 121001, 2017.

[14] H. Damerau, A. Funken, R. Garoby, S. Gilardoni, B. Goddard, K. Hanke, A. Lombardi, D. Manglunki, M. Meddahi, B. Mikulec, G. Rumolo, E. Shaposhnikova, M. Vretenar, J. Coupard (eds.), "LHC Injectors Upgrade, Technical Design Report, Vol. I: Protons", CERN-ACC-2014-0337, 2014.